

Ultrasonic attenuation in cesium for oblique magnetic fields*

J. Trivisonno

*Department of Physics, John Carroll University, † Cleveland, Ohio 44118
and Department of Physics, University of Arizona, Tucson, Arizona 85721*

G. Kaltenbach

B. F. Goodrich Company, Akron, Ohio

(Received 8 April 1974; revised manuscript received 17 October 1974)

The ultrasonic attenuation of longitudinal waves was measured in cesium single crystals in oblique and transverse magnetic fields. Ultrasonic frequencies between 10 and 90 MHz were employed and the attenuation was studied at 4.2 and 1.5 °K. For an angle of 55 deg between the direction of propagation and the magnetic field direction, the change in the attenuation between zero-field value and the limiting high-field value is a direct measure of the zero-field electronic contribution to the ultrasonic attenuation. Ultrasonic absorption edges which occur in oblique magnetic fields were also studied. The results are compared with the free-electron theory.

I. INTRODUCTION

The alkali metals, potassium in particular, have been the subject of numerous ultrasonic experiments.¹ Fermi-surface dimensions have been reported, and detailed comparisons of the magnetic field dependence of the attenuation with the free-electron theory have been made. No reliable value of the zero-field electronic contribution to the attenuation, however, has been reported. For $ql \ll 1$, data obtained on polycrystalline potassium² indicate that the electronic contribution to the attenuation as determined from the temperature dependence of the attenuation is considerably larger (60%) than the free-electron value. The results in single-crystal potassium, however, obtained from oblique-field measurements³ at 60 MHz ($ql \sim 11$) appear to be in agreement with the free-electron theory.

Detailed studies of the ultrasonic attenuation in cesium single crystals have been reported both for the case of longitudinal waves⁴ and for shear waves.⁵ In both studies the attenuation was measured in transverse magnetic fields. The first study dealt with the magnetoacoustic effect in transverse magnetic fields using longitudinal waves. The period of the geometric oscillations was used to measure directly the radial anisotropy in the (100) and (110) planes. The results indicate that the Fermi surface of cesium bulges in the [110] directions by 4% and is depressed in the [100] and [111] directions by about 1%. A detailed study of the magnetic field dependence of the attenuation showed that, while the positions of the extrema of the oscillations are in excellent agreement with the free-electron theory, a variation in signal amplitude with magnetic field direction was observed and the overall attenuation curves differed from theory. While the attenuation did saturate at high fields as $1/H^2$ for all orientations of the magnetic

field, an anisotropy in the high-field attenuation was observed. A later study using shear waves exhibited similar behavior, and a less than linear frequency dependence in the shear-wave attenuation was observed. With the exception of the deviations listed above, the results for both studies were quite free-electron-like.

The present study extends the measurements of longitudinal waves to the case where the magnetic field is at an arbitrary angle with respect to the direction of propagation. The ultrasonic attenuation of longitudinal waves in oblique magnetic fields³ has been calculated in detail for the free-electron model using the Cohen, Harrison, and Harrison formalism.⁶ The main aspect of this theory of the attenuation in oblique magnetic fields that relates to the present study is the calculation which shows that the electronic contribution to the attenuation at high fields vanishes when the angle between the direction of propagation and the magnetic field is in the vicinity of 55°.

If this is the case, measurements of the attenuation changes in oblique magnetic fields provide a way of directly determining the zero-field electronic contribution to the ultrasonic attenuation. The electronic contribution to the attenuation in the absence of a magnetic field in nonsuperconductors is difficult to measure. Changes in the attenuation with magnetic field, however, are readily measured. In typical ultrasonic experiments, the magnetic field is applied perpendicular to the direction of propagation and the change in attenuation with field is used to sort out the electronic portion of the total attenuation. For this geometry the change in the attenuation between the zero-field value and the limiting high-field value is given by

$$\Delta \alpha_{90^\circ} = \alpha_E(0) - \alpha_E(H),$$

where $\alpha_E(0)$ is the zero-field electronic contribution to the attenuation and $\alpha_E(H)$ is the limiting high-field attenuation. Neither $\alpha_E(0)$ nor $\alpha_E(H)$ are directly measured.

For the case where the magnetic field is at an angle of 55° with respect to the direction of propagation, the change in the attenuation with field is given by

$$\Delta\alpha_{55^\circ} = \alpha_E(0) - \alpha_E(H, 55^\circ).$$

If the high-field attenuation, $\alpha_E(H, 55^\circ)$, vanishes, then the change in the attenuation is a direct measure of the zero-field electronic contribution to the attenuation. Measurements in oblique and transverse fields then yield directly both $\alpha_E(0)$ and $\alpha_E(H)$, and these measurements can be compared directly with the predictions of the free-electron theory.

The ultrasonic attenuation in the absence of a magnetic field assumes a simple form in the free-electron model. Pippard⁷ has derived the following expression which is valid for arbitrary values of ql and for the case of isotropic scattering:

$$\alpha_E(0) = \frac{1}{6} \pi (Nm V_F / \rho V_s) q F(ql), \quad (1)$$

where

$$F(ql) = \frac{6}{\pi} \frac{ql}{3} \left(\frac{\tan^{-1} ql}{ql - \tan^{-1} ql} - \frac{3}{q^2 l^2} \right),$$

where m is the electron mass, V_F is the Fermi velocity, ρ is the density, l is the electron mean free path, and q is the sound wave number. This expression assumes a simple form in two limiting cases. For $ql \ll 1$, $F(ql) = (8/5\pi)ql$ and

$$\alpha_E(0) = \frac{4}{15} (Nm V_F / \rho V_s) q^2 l, \quad (2)$$

and for $ql \gg 1$, $F(ql) = 1$, and

$$\alpha_E(0) = \frac{1}{6} \pi (Nm V_F / \rho V_s) q. \quad (3)$$

In this region the attenuation is proportional to the frequency and independent of the electron mean free path. This feature allows a direct comparison of experiment and theory without any adjustable parameters.

In a large magnetic field applied perpendicular to \hat{q} , the attenuation for arbitrary ql values is given by

$$\alpha_E(H) = \frac{1}{15} (Nm V_F / \rho V_s) q^2 l. \quad (4)$$

The limiting high-field attenuation in a transverse magnetic field thus has the same frequency dependence and mean-free-path dependence as the zero-field attenuation in the local limit. The present paper reports for cesium the results of measurements of the attenuation of longitudinal waves in oblique and transverse magnetic fields over a wide

range of ql values. The results for $\alpha_E(0)$ and $\alpha_E(H)$ and their temperature dependences are compared directly with the predictions of the free-electron theory.

For oblique magnetic fields, ultrasonic absorption edges in the attenuation occur. Results of these measurements are also presented and compared with the free-electron model and the previous measurements obtained in potassium.

II. EXPERIMENTAL ASPECTS

The techniques used to grow the single crystals and prepare the acoustic specimens were the same as used in our previous studies. Some relevant data for the crystals for which data are reported are shown in Table I. The lengths are room-temperature measurements made with a micrometer. The velocities were measured at 4.2°K and at a frequency of 10 MHz prior to taking the attenuation data. For the data taken on oriented crystals, the values listed are consistent with the more accurate data obtained in the study of the single-crystal elastic constants of cesium⁸ where a buffer technique was employed.

Two X-cut transducers with a fundamental frequency of 10 MHz cemented on opposite ends of the acoustic specimen were used to generate and detect the acoustic signals. The specimen was mounted in a spring-loaded ultrasonic probe which fit into a 1.5-in.-diam tail of a helium Dewar that was suspended between the pole faces of a 12-in. Harvey Wells magnet. The probe was oriented in such a manner that the magnetic field could be rotated from a direction parallel to the direction of propagation \hat{q} to a direction perpendicular to \hat{q} .

An ultrasonic pulse-echo technique employing phase-sensitive detection⁹ was used to measure the attenuation. Direct X-Y recorder plots of the attenuation as a function of magnetic field were obtained for various orientations of \hat{H} relative to \hat{q} . For $\hat{H} \perp \hat{q}$, oscillations in the low-field attenuation were obtained for all frequencies between 10 and 90 MHz at 1.5°K which are indicative of relatively high ql values. For θ near 55° , expanded sweeps were used to accurately locate the position of the absorption edge. Much of the data, however,

TABLE I. Crystal length, orientation, and sound velocity for four cesium samples.

Crystal	L (cm)	\hat{q}	V_s (10^5 cm/sec)
I	0.570	[111]	1.45
II	0.691	[110]	1.40
III	0.735	[110]	1.42
IV	0.686	random	1.32

were taken in a field of 15 kG as the angle between the magnetic field and the direction of propagation was varied. The extrema in the attenuation-vs-angle plots were accurately located by increasing the gain of the phase-sensitive detector. The extrema occur for $\hat{H} \parallel \hat{q}$ ($\theta=0^\circ$), $\hat{H} \perp \hat{q}$ ($\theta=90^\circ$), and for $\theta=55^\circ$. Data were then taken for every 5° interval between $\theta=0^\circ$ and $\theta=90^\circ$. The attenuation was measured relative to the zero-field attenuation. No amplitude-dependent attenuation effects were observed, and amplitude-independent effects which are temperature dependent are not important for data obtained in the manner described above. Measurements were made for ultrasonic frequencies between 10 and 90 MHz and for temperatures between 4.2 and 1.5°K.

III. RESULTS

A. Ultrasonic attenuation in oblique magnetic fields

A typical rotation diagram of the attenuation in a 15 kG magnetic field is shown in Fig. 1. The limiting high-field attenuation relative to the zero-field attenuation is plotted as a function of the angle between \hat{H} and \hat{q} . For these data, \hat{q} is along the [111] direction, the frequency is 50 MHz, and the temperature is 4.2°K. The dashed line indicates the value of the zero-field attenuation. For $\hat{H} \parallel \hat{q}$, the high-field attenuation is equal to the zero-field attenuation, a result consistent with the free-electron theory. As the angle between \hat{H} and \hat{q} is increased, the high-field attenuation decreases and reaches a minimum, which is quite broad, at an angle of approximately 55° . As θ is increased

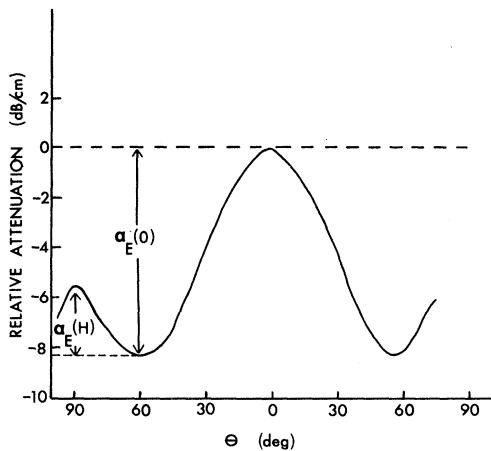


FIG. 1. Plot of the relative attenuation in dB/cm vs angle for a field of 15 kG. The attenuation is measured relative to the zero-field attenuation, and θ is the angle between \hat{H} and \hat{q} . The data are for $\hat{q} \parallel [111]$, $f=50$ MHz, and $T=4.2^\circ\text{K}$.

further, a maximum in the attenuation occurs for $\theta=90^\circ$, $\hat{H} \perp \hat{q}$. The difference in the attenuation between the zero-field attenuation and the value of the high-field attenuation at the minimum, $\theta=55^\circ$, is assumed to be a measure of $\alpha_E(0)$, the zero-field electronic contribution to the attenuation. The difference in the attenuation between the minimum 55° and maximum, at $\theta=90^\circ$, is then a measure of $\alpha_E(H)$. The free-electron theory predicts that $\alpha_E(H)$ is less than $\alpha_E(0)$ for $ql < 6.8$ and greater than $\alpha_E(0)$ for $ql > 6.8$. Thus, according to the free-electron theory, the data shown in Fig. 1 correspond to $ql < 6.8$.

The effect of varying the temperature and thereby the electron mean free path is shown in Fig. 2. The temperature is 1.5°K, and the general features of the plot are similar to those in Fig. 1. The attenuation at $\theta=90^\circ$, $\alpha_E(H)$, is now larger than $\alpha_E(0)$ and has increased by nearly a factor of 4 while $\alpha_E(0)$ has increased by only 10%.

The effect of varying the ultrasonic frequency for a fixed temperature of 1.5°K is shown in Figs. 2-4. In Fig. 3, the frequency is 30 MHz, and $\alpha_E(H)$ is seen to be approximately equal to $\alpha_E(0)$, corresponding to a free-electron value of ql of 6.8. The attenuation $\alpha_E(0)$ obtained from these data at $\theta=55^\circ$ is also seen to be roughly three-fifths of the corresponding attenuation measured at 50 MHz. That is, the attenuation change measured at $\theta=55^\circ$ is proportional to the ultrasonic frequency. (The stronger dependence of $\alpha_E(H)$ on frequency is evident.) Similar data, illustrating the frequency dependence of $\alpha_E(0)$ and $\alpha_E(H)$, are shown in Fig. 4 for an ultrasonic frequency of 70 MHz. The increases in $\alpha_E(0)$ and $\alpha_E(H)$ are clearly evident. Not only has the attenuation $\alpha_E(H)$ increased by a factor of 2 from its value at 50 MHz,

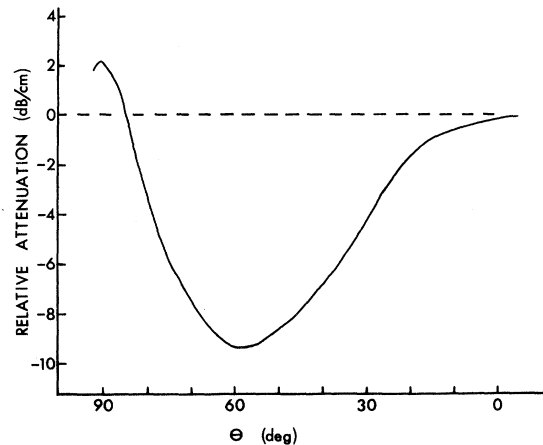


FIG. 2. Relative attenuation vs angle for $\hat{q} \parallel [111]$, $f=50$ MHz, and $T=1.5^\circ\text{K}$.

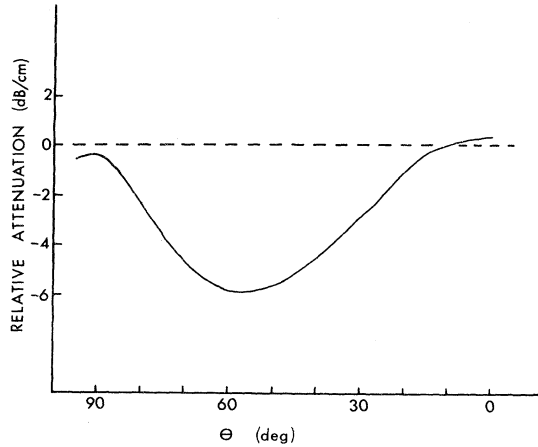


FIG. 3. Relative attenuation vs angle for $\hat{q} \parallel [111]$, $f = 30$ MHz, and $T = 1.5$ °K.

but the attenuation near 90° now is very sharply peaked, in contrast to the results obtained at lower ql values. The high-field attenuation for θ near 90° becomes even more sharply peaked at higher ql values. For large ql values therefore the magnetic field must be accurately aligned perpendicular to \hat{q} when measuring $\alpha_E(H)$. This point has been stressed in a recent paper by Cox and Gavenda.¹⁰ As mentioned earlier, $\alpha_E(H)$ in cesium was found to be anisotropic as \hat{H} was rotated in a plane perpendicular to \hat{q} , with the maximum anisotropy being 15%. In a metal as difficult to handle as cesium, some of the observed anisotropy probably can be attributed to misorientation effects. Since anisotropy is also observed at low ql values, this effect, however, cannot be attributed entirely to misorientation. A slight anisotropy in $\alpha_E(H)$ for potassium has also been observed.¹⁰ This anisotropy in $\alpha_E(H)$, of course, represents a departure from the free-electron theory. Since the deviations are small, we shall assume in the

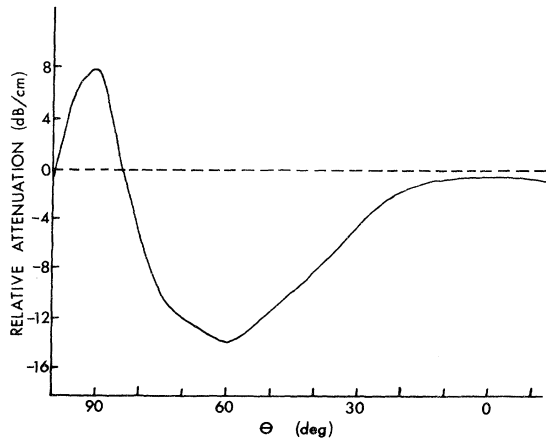


FIG. 4. Relative attenuation vs angle for $\hat{q} \parallel [111]$, $f = 70$ MHz, and $T = 1.5$ °K.

analysis of the data that the free-electron theory holds for the purpose of estimating ql values. In any case, for large ql values $\alpha_E(0)$ is not dependent on the choice of ql .

The experimental values of $\alpha_E(0)$ and $\alpha_E(H)$ taken from the high-field rotation plots are listed in Table II for a number of crystals. The experimental values of $\alpha_E(0)$ are accurate to about 1 dB/cm. The values of $\alpha_E(H)$ are accurate to 1 dB/cm at low frequencies and 2 dB/cm at the highest frequency shown for each crystal. At high ql values the signal-to-noise ratio and the sensitivity are poor for the attenuation measured in transverse magnetic fields. The frequencies listed are accurate to ± 1 MHz, and the data shown in this table were obtained from measurements at 1.5 °K. For each crystal, $\alpha_E(0)$, within experimental error, exhibits a linear frequency dependence, while $\alpha_E(H)$ is proportional to the square of the frequency. The ql values listed were chosen by looking for the frequency for which $\alpha_E(0)$ equals $\alpha_E(H)$, corresponding to $ql = 6.8$, and then scaling ql with frequency. These ql values were then used to obtain the theoretical values of $\alpha_E(H)$, which is proportional to q^2l , and were also used to calculate $F(ql)$ and thus $\alpha_E(0)$. Since $F(ql)$ is a slowly varying function of ql for $ql > 7$, the choice of ql is not critical, and the theoretical values of $\alpha_E(0)$, particularly at the higher frequencies, are independent of l . A direct comparison between experiment and theory for $\alpha_E(0)$ is then possible without any adjustable parameters. Not only are the experimental values of $\alpha_E(0)$ obtained from oblique-field measurement seen to exhibit the proper frequency dependence expected at large ql values, but also the magnitude of the attenuation is in good agree-

TABLE II. Comparison of experimental and theoretical values of the zero-field attenuation $\alpha_E(0)$ and the limiting-high-field attenuation $\alpha_E(H)$. The experimental values are for $T = 1.5$ °K.

Crystal	f (MHz)	Experimental		Theoretical		ql
		$\alpha_E(0)$ (dB/cm)	$\alpha_E(H)$ (dB/cm)	$\alpha_E(0)$ (dB/cm)	$\alpha_E(H)$ (dB/cm)	
I	30	5.8	5.4	5.1	4.3	5.4
	50	9.5	11.6	9.2	12.0	9.0
	70	13.9	22.0	13.1	23.5	12.6
II	10	2.0	1.1	1.6	0.9	3.3
	30	7.4	9.8	6.1	8.6	10.0
	50	11.2	22.2	10.7	23.9	16.7
III	30	7.1	6.8	5.6	5.5	6.6
	50	13.1	18.4	10.0	15.5	11.0
	70	18.4	31.4	14.6	30.0	15.4
IV	10	1.6	1.0	1.7	0.8	2.5
	30	6.4	7.3	6.7	7.2	7.5
	50	11.8	20.4	11.7	20.2	12.5
	70	15.1	37.4	16.9	39.5	17.5

ment with theory. In fact, for the crystal with $\hat{q} \parallel [111]$, the results for $\alpha_E(0)$ and for $\alpha_E(H)$ for the ql values listed are in excellent agreement with free-electron theory. For $\hat{q} \parallel [110]$, the experimental values of $\alpha_E(0)$ are consistently higher than the corresponding theoretical values, and adjusting ql will not affect the theoretical values at the higher frequencies. The theoretical values of $\alpha_E(0)$ and $\alpha_E(H)$ which contain the frequency and square of the sound velocity are accurate to about 6%. The experimental results for crystal III indicate that the attenuation for $\hat{q} \parallel [110]$ is slightly (5–10)% higher than the free-electron value. Unfortunately, we were not able to make measurements for $\hat{q} \parallel [100]$ since no single crystals were grown with a $[100]$ direction near the boule axis. A study of unoriented single crystals was also made, and the results for one of these are shown in Table II. The data in every respect are similar to data obtained for $\hat{q} \parallel [111]$ and $\hat{q} \parallel [110]$, and despite the fact the wave is quasilongitudinal the results are in excellent agreement with the free-electron theory for longitudinal waves. The data listed in Table II indicate that the ultrasonic attenuation measured in a large oblique magnetic field gives a direct measure of the zero-field electronic contribution to ultrasonic attenuation, and, with the exception of the minor deviations for $\hat{q} \parallel [110]$, the results are in excellent agreement with the free-electron theory.

For each crystal, the temperature dependence of $\alpha_E(H)$ and $\alpha_E(0)$ for a given ultrasonic frequency was measured as the temperature was varied between 4.2 and 1.5 °K. The experimental and theoretical values of $\alpha_E(0)$ and $\alpha_E(H)$ at 4.2 °K are listed in Table III, and the corresponding values at 1.5 °K are repeated for clarity.

Since $\alpha_E(H)$ is proportional to the electron mean free path for arbitrary ql values, the temperature dependence of the electron mean free path due to phonon scattering can be obtained from measurements of the temperature dependence of $\alpha_E(H)$. The results have been reported earlier.¹¹ The mean free path essentially varies as T^5 for $T < 2.5$ °K and as $T^{3.5}$ for $T > 3$ °K. In general, l increases by a factor of 4–6 over this temperature range for the crystals used in our studies. This increase in the mean free path is consistent with residual resistance measurements made on cesium single-crystal boules between 4.2 and 1.5 °K using an eddy-current technique.¹² The ratio of the mean free paths obtained from the measured value of $\alpha_E(H)$ at 4.2 and 1.5 °K was used to obtain the ql values at 4.2 °K, which are listed in Table II. The appropriate ql value was then used to calculate $F(ql)$ and the theoretical value of $\alpha_E(0)$. The experimental values of $\alpha_E(0)$ do not exhibit the

large changes expected as calculated from the Pippard function $F(ql)$, at least for the ql values used. This function, however, was derived under the assumption that the mean free path is impurity limited. The electron mean free path in this experiment is clearly phonon-limited at 4.2 °K and becomes impurity limited at 1.5 °K. Bhatia and Moore¹³ have obtained expressions for the ultrasonic attenuation in the free-electron model by solving the Boltzman equation without assuming the existence of a relaxation time. The collision integral in this equation is assumed to arise from the interactions of electrons with thermal phonons as well as from impurities. For the case of isotropic scattering, their expressions are identical to those observed by Pippard. For the more general case, the acoustic attenuation exhibits a ql dependence which differs from that given by Pippard. In the local limit, the attenuation is proportional to an effective relaxation time τ_2 , which involves different angular weighting factors than the relaxation time associated with the electrical conductivity τ_1 . The attenuation, however, is given by the same expression as derived by Pippard if τ_2 is used rather than τ_1 . For the extreme non-local limit, the attenuation is independent of relaxation time, in agreement with the Pippard result. For arbitrary ql values, however, the attenuation must be calculated numerically. The ratio of the attenuation to the limiting attenuation will in general deviate slightly from the Pippard results. Peverley¹⁴ also has obtained expressions for the attenuation with no restriction on locality, and these results are equivalent to those obtained in Ref. 13. The attenuation was evaluated for somewhat artificial models and shows deviations from Pippard's results for intermediate ql values. The magnitude of the deviations depends critically on the directional properties of the scattering cross section. If appreciable backward scattering is

TABLE III. Experiment values of $\alpha_E(0)$ and $\alpha_E(H)$ at 4.2 and 1.5 °K and the corresponding theoretical values.

Crystal	f (MHz)	Experimental		Theoretical		ql
		$\alpha_E(0)$ (dB/cm)	$\alpha_E(H)$ (dB/cm)	$\alpha_E(0)$ (dB/cm)	$\alpha_E(H)$ (dB/cm)	
I	50	8.4	2.8	6.6	2.9	2.2
	50	9.5 ^a	11.6 ^a	9.2 ^a	12.0 ^a	9.0
II	50	10.6	4.1	8.3	4.6	3.2
	50	11.2 ^a	22.2 ^a	10.7 ^a	23.9 ^a	16.7
III	70	15.5	6.5	10.7	6.3	3.0
	70	18.4 ^a	31.4 ^a	14.6 ^a	30.0 ^a	15.4
IV	70	14.0	6.7	13.0	7.1	3.1
	70	15.1 ^a	37.4 ^a	16.9 ^a	39.5 ^a	17.5

^a Values for $T = 1.5$ °K.

present, large anomalies in the attenuation are predicted. No anomalies have been observed for the data obtained in the present experiments for the ql range studied. However, some of the attenuation curves shown in Ref. 14 for the case where backward scattering is included exhibit a ql dependence which can easily account for the data shown in Table III. That is, the attenuation essentially approaches a limiting value at lower ql . The ql dependence of the zero-field attenuation clearly warrants further study. Measurements of $\alpha_E(0)$ over a wide frequency range at lower ql values in particular would be desirable. Measurements of the temperature dependence of $\alpha_E(0)$ in the local limit obtained from oblique-field measurements would also be of interest.

B. Ultrasonic absorption edges

The large decrease in the ultrasonic attenuation in oblique magnetic fields is associated with the occurrence of ultrasonic absorption edges. While the attenuation is independent of magnetic field for $\hat{H} \parallel \hat{q}$, as the angle between \hat{H} and \hat{q} is increased ultrasonic absorption edges appear in the attenuation-vs-magnetic-field sweeps. These edges were measured in several crystals at 1.5°K at 70 and 90 MHz. The corresponding ql values ranged between 16 and 24, which is considerably higher than the ql values obtained in the earlier study in potassium. The edges at these ql values are readily detected for $\theta < 60^\circ$. For angles greater than 60° the low-field attenuation is dominated by geometric oscillations associated with nonexternal orbits. The last oscillation makes it difficult to locate the edge position.

Because ultrasonic absorption edges in the ultrasonic attenuation have been discussed in detail by a number of investigators,^{15,16} only a brief discussion will be given. Briefly, since the velocity of electrons in a magnetic field is a periodic function of time, the velocity can be expressed as a Fourier series. The strength of the interaction between the electron and the force field of the sound wave is proportional to the Fourier coefficient of the velocity. An interaction can occur whenever $\omega_c = \vec{q} \cdot \vec{V}^0$, where ω_c is the cyclotron frequency and \vec{V}^0 is the $N=0$ Fourier component of the velocity in the direction of the magnetic field. For $\hat{H} \parallel \hat{q}$, there is no Fourier component of the velocity which is a function of H for electrons on a spherical Fermi surface; so the attenuation is independent of magnetic field. This is exactly what is observed. For oblique angles, other Fourier components enter and absorption edges can occur. The position of the edge is given by $\omega_c = \vec{q} \cdot \vec{V}_m^0$, where V_m^0 is the maximum electron velocity parallel to the magnetic field. The value of the magnet-

tic field, H_c at the edge position, together with the measured sound velocity and ultrasonic frequency, can be used to compute $m_c^* V_m^0$, where m_c^* is the cyclotron mass. Detailed calculations of the attenuation near H_c have been carried out in Ref. 3 both for the free-electron model and for the spin-density model.¹⁷ For low ql values ($ql < 50$), the theoretical plots for the spin-density model and the free-electron model are indistinguishable. The position of the absorption edge for the spin-density model will, however, occur at a lower magnetic field. The experimental data in potassium appear to favor the free-electron model.

Figure 5 shows the negative of the derivative of the amplitude attenuation coefficient with respect to magnetic field plotted as a function of H for $\theta = 49^\circ$ and $\theta = 52^\circ$. The peak in these plots corresponds to the inflection point in the attenuation-vs-magnetic-field plots and corresponds to the edge position. The curves are quite similar to the results reported for potassium.

In Table IV, the data obtained for two of the crystals studied are summarized. The results are expressed as $H_c V_s / f \cos \theta$, the measured quantities. The free-electron value of this quantity is 26.7 G cm. For both crystals, within experimental uncertainty of about 6%, agreement with the free-electron theory is obtained. For crystal IV the orientation of \hat{H} with respect to the crystallographic axes was not known. For crystal III the axis of rotation of \hat{H} is near a $[110]$ direction, so that for $\theta = 55^\circ$ \hat{H} is approximately along the $[112]$ direction. In this direction the curvature of the Fermi surface is spherical. In any case $H_c / \cos \theta$ is essentially constant, indicating that V_m^0 is constant for the θ values shown. The experiments done in ce-

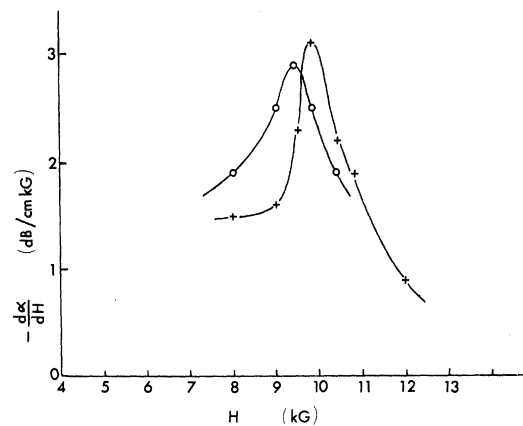


FIG. 5. Plot of the negative of the derivative of the amplitude attenuation coefficient, $-d\alpha/dH$, as a function of magnetic field. The crosses are for $\theta = 49^\circ$ and the open circles for $\theta = 52^\circ$.

TABLE IV. Frequency and angular dependence of the ultrasonic absorption edges. H_c is the value of the magnetic field at the edge. $H_c V_s / f \cos \theta = 2\pi m V_m C / e$ has a free-electron value of 26.7 G cm.

Crystal	f (MHz)	θ (deg)	H_c (kG)	$H_c V_s / f \cos \theta$ (G cm)	$(d\alpha/dH)_{\max}$ (dB/kG cm)
III	70	53	8.00	27.0	3.0
	70	55	7.50	26.5	3.7
	70	58	7.14	27.4	4.2
IV	70	49	9.80	28.3	3.1
	70	52	9.38	28.7	2.9
	70	60	7.40	27.9	6.8
	90	54	11.0	27.4	3.8
	90	59	10.1	28.7	7.3

sium therefore lend no support to the existence of a spin-density or charge-density wave ground state in cesium.

CONCLUSION

The attenuation measured in oblique magnetic fields appears to be a direct measure of the zero-field electronic contribution to the ultrasonic attenuation. Additional measurements in the local limit in particular would be desirable. In this limit, the zero-field attenuation is proportional to τ_2 . Combined measurements of the attenuation and electrical resistivity therefore give a direct

measure of τ_2/τ_1 . The ratio, as pointed out by Rice and Sham,¹⁸ is quite sensitive to the relative amounts of normal and umklapp scattering and to the choice of the pseudopotential used in the calculations. The measurements therefore provide a critical test of the shape of the pseudopotential used to calculate the electron-phonon interaction. Potassium, rather than cesium, is the logical choice for detailed studies. From an experimental point of view potassium is much easier to handle than cesium. In addition, accurate resistivity data^{19,20} are available, and a number of theoretical calculations^{20,21} based on a realistic phonon spectrum have been made. Ultrasonic attenuation measurements on potassium, similar to these reported for cesium, should provide a clearer understanding of electron-phonon interactions in the alkali metals and, together with resistivity data, should enhance our understanding of the role of umklapp scattering in electron-phonon interactions.

ACKNOWLEDGMENTS

We are extremely grateful to Professor R. W. Stark for many valuable discussions and to Ronald Reifenberger for his comments and aid. The comments of Professor D. E. Schuele are also gratefully acknowledged. One of us (J.T.) would like to acknowledge the hospitality of the Physics Department of the University of Arizona, where this manuscript was prepared.

*Work supported by NSF Grant No. GH-31652.

†Permanent address.

¹J. Mertsching, Phys. Status Solidi **37**, 465 (1970), and references contained therein.

²G. G. Natale and I. Rudnick, Phys. Rev. **167**, 687 (1968).

³M. P. Greene, A. R. Hoffman, A. Houghton, and J. J. Quim, Phys. Rev. **156**, 798 (1967).

⁴J. Trivisonno and J. A. Murphy, Phys. Rev. B **1**, 3341 (1970).

⁵B. Keramidas, J. Trivisonno, and G. Kaltenbach, Phys. Rev. B **6**, 4412 (1972).

⁶M. H. Cohen, M. J. Harrison, and W. A. Harrison, Phys. Rev. **117**, 936 (1960).

⁷A. B. Pippard, Philos. Mag. **41**, 1104 (1955).

⁸F. J. Kollarits and J. Trivisonno, J. Phys. Chem. Solids **29**, 2133 (1968).

⁹J. Davenport, J. L. Hunter, and R. A. Leskovec, Rev. Sci. Instrum. **41**, 1426 (1970).

¹⁰W. Royall Cox and J. D. Gavenda, Phys. Rev. B **3**,

324 (1971).

¹¹J. Trivisonno and G. Kaltenbach, Solid State Commun., **15**, 367 (1974).

¹²C. P. Beam, R. W. DeBlois, and L. B. Nesbitt, J. Appl. Phys. **30**, 1976 (1959).

¹³A. B. Bhatia and R. A. Moore, Phys. Rev. **121**, 1075 (1961).

¹⁴J. Roger Peverley, Phys. Rev. Lett. **31**, 886 (1973).

¹⁵B. K. Jones, Philos. Mag. **9**, 217 (1964).

¹⁶R. W. Stark, J. Trivisonno, and R. Schwarz, Phys. Rev. B **3**, 2465 (1971).

¹⁷A. W. Overhauser, Phys. Rev. Lett. **13**, 19 (1964); Phys. Rev. **128**, 1437 (1962).

¹⁸T. M. Rice and L. J. Sham, Phys. Rev. B **1**, 4546 (1970).

¹⁹J. W. Ekin and B. W. Maxfield, Phys. Rev. B **4**, 4215 (1971).

²⁰D. Guban, Proc. R. Soc. A **325**, 223 (1971).

²¹P. M. Trofimenkoff and J. W. Ekin, Phys. Rev. B **4**, 2392 (1971).